Atmos. Meas. Tech. Discuss., 4, 7597–7622, 2011
www.atmos-meas-tech-discuss.net/4/7597/2011/
doi:10.5194/amtd-4-7597-2011

Atmospheric Measurement Techniques Discussions

Aerosol optical depth retrieval in the Arctic region using MODIS based on prior knowledge

L. Mei[1,8], Y. Xue[1,2], G. de Leeuw[3,4,5], T. Hou[6,8], J. Guang[1], L. Yang[7], Y. Li[1,8], H. Xu[1,8], and X. He[1,8]

[1]State Key Laboratory of Remote Sensing Science, Jointly Sponsored by the Institute of Remote Sensing Applications of Chinese Academy of Sciences and Beijing Normal University, Institute of Remote Sensing Applications, Chinese Academy of Sciences, Beijing 100101, China
[2]Faculty of Computing, London Metropolitan University, 166-220 Holloway Road, London N7 8DB, UK
[3]Department of Physics, University of Helsinki, Helsinki, Finland
[4]Finnish Meteorological Institute, Climate Change Unit, Helsinki, Finland
[5]Netherlands Organisation for Applied Scientific Research TNO, Utrecht, The Netherlands
[6]Center for Earth Observation and Digital Earth of the Chinese Academy of Sciences, Beijing 100094, China

[7] School of Geography, Beijing Normal University, Beijing 100875, China
[8] Graduate University of the Chinese Academy of Sciences, Beijing 100049, China

Received: 19 October 2011 – Accepted: 8 December 2011 – Published: 19 December 2011

Correspondence to: Y. Xue (yxue@irsa.ac.cn)

Published by Copernicus Publications on behalf of the European Geosciences Union.

Abstract

The Arctic is especially vulnerable to the long-term transport of aerosols and other pollutants because aerosols can affect the albedo of the surface by deposition on snow and ice. However, aerosol observations for this area are sparse and hence there is considerable uncertainty in the knowledge on the properties of the Arctic aerosol. Arctic aerosol observations are needed to fill this gap because these are among the basic and most important parameters for researching the Arctic environment. Atmospheric remote sensing using satellites offers us an opportunity to describe the aerosol distribution in terms of both local, regional and global coverage. However, AOD retrieval over a bright surface remains a difficult task because it is hard to separate and explicitly describe the contribution of the observed signal reflected by the variable surface and back scattering by the semi-transparent aerosols, especially with a large solar or sensor zenith angle. In this paper, an approach using a synergetic approach with Moderate Resolution Imaging Spectroradiometer (MODIS) data based on prior knowledge is presented. The detailed analysis of the model demonstrates that it is suitable for Arctic region AOD retrieval. Six AERONET stations at high latitude (Andenes, Barrow, Ittoqqortoormiit, OPAL, Thule, and Tiksi) were used for validation, and the correlation coefficient between retrieved AODs and AERONET AODs was 0.75 and the retrieval absolute error is approximately 0.1, while the relative error is 20 % (at some stations with clear skies as low as 10 % was found). Furthermore, the Russian wildfires that occurred in late July of 2010 and their effect on the Arctic environment is presented; Satellite retrieved AODs in the Arctic increased to 1.0 during 1 August and 15 August 2010, even 2.0, during the burning phase, and subsequently returned to normal values (lower than 0.1), which was fully in line with the AERONET observations. This indicates that the fire plumes were transported to the Arctic region.

1 Introduction

The Arctic environment, especially the atmosphere, is a significant indicator of global change. Satellite observations and Lidar measurements have revealed the occurrence of substantial amounts of smoke and other particulate matter in the tropopause region and lower stratosphere at high latitudes and in the Arctic region (Damoah et al., 2004) due to transport of anthropogenic (Shaw, 1995) or natural aerosol produced by sources, such as wildfires (Kim et al., 2005) and volcanic eruptions (Herber et al., 1996). Long-range transport over continental, intercontinental and even global distances is the dominant pollution source in the Arctic region. The Arctic haze in spring (Ackerman et al., 1986) and biomass burning during summer play predominant roles in both the distribution of solar radiation and the total energy balance in the Arctic. Research to better understand changes in arctic atmospheric composition and climate is urgently needed.

Ground-based observation is the primary method for atmospheric environment research in the Arctic. Many research campaigns, such as the Arctic Gas and Aerosol Sampling Programme (AGASPI), the Arctic Boundary Layer Expedition (ABLE) 3A and 3B campaigns, Arctic Research of the Composition of the Troposphere from Aircraft and Satellites (ARCTAS), and the Canadian Arctic Validation Campaign (ACE), have been conducted or are planned to be conducted by scientists to collect data at ground-based stations in order to get better information on the aerosol properties. However, this information applies to local areas. Information on long-range transport of particles to the Arctic is mainly obtained from model simulation. Satellite remote sensing would provide a complementary source of information. However, parameters such as aerosol optical depth (AOD) are hard to retrieve at high latitudes such as the polar area. Therefore, aerosol remote sensing remains underutilised in the Arctic region (Istomina et al., 2011). The lack of a satellite AOD product in the Arctic region can be attributed to the imperfection of retrieval theories, as well as the special under-surface and location of the Arctic region. In fact, the bright surface caused by ice and snow and a large solar zenith angle is exactly the bottleneck of AOD retrieval.

AMTD
4, 7597–7622, 2011

One of the crucial issues when retrieving aerosol properties using satellite images is separating and explicitly describing the contribution to the radiation observed at the top of the atmosphere (TOA) by the radiation reflected at the variable surface and backscattering by semi-transparent aerosols, corresponding with the determination of the surface reflectance characteristics and the aerosol properties (Hsu et al., 2004; Martonchik, 2009; Govaerts et al., 2010). However, the problem is ill-posed and it is still a challenge in the research of atmospheric and land applications, especially when the retrieval occurs above bright surfaces such as snow and ice. The contribution of aerosols observed by satellites is very small as compared to the surface contribution, making the retrieval of aerosol properties uncertain.

Algorithms for aerosol retrieval over land have been developed for different sensors, for instance, the European Space Agency (ESA) MEdium Resolution Imaging Spectrometer (MERIS) algorithm for MERIS (Santer et al., 1999), the Along-Track Scanning Radiometer(ATSR-2) dual view algorithm (ADV) (Veefkind et al., 1998), the Advanced ATSR (AATSR) algorithm for AATSR (Grey et al., 2006), the Jet Propulsion Laboratory (JPL) algorithm for Multiangle Imaging Spectroradiometer (MISR) (Diner et al., 2005), the Dark Dense Vegetation (DDV) algorithm (Kaufman et al., 1997; Remer et al., 2006) and the DeepBlue algorithm (Hsu et al., 2004) for Moderate Resolution Imaging Spectroradiometer (MODIS), the Centre National d'EtudesSpaciales (CNES) algorithm (Deuze et al., 2001) for POLarization and Directionality of the Earth's Reflectance instrument (POLDER) and optimal estimation for Meteosat Second Generation – Spinning Enhanced Visible and Infrared Imagers (MSG/SEVIRI) (Govaerts et al., 2010). All of the algorithms above are suitable for certain ground surface conditions. However, there are no retrieval products over very reflective snow and ice surfaces and also highly reflective surfaces such as the Sahara desert pose a problem for some of the algorithms. For example, one major limitation of the MODIS Dense Dark Vegetation (DDV) approach is that no retrievals are performed when the surface reflectance at 2.1-µm is above 0.15, and the assumption of transparency in this channel does not apply (Kaufman et al., 1997; Hsu et al., 2004; Remer et al., 2005). Even though the

AMTD

4, 7597–7622, 2011

relationship of visible to 2.12-µm surface reflectance is improved as a function of geometry, surface type (Remer et al., 2001; Gatebe et al., 2001) and scattering angle (Levy et al., 2007), this approach is still not effective for bright surfaces. Hsu et al. (2004) described a new approach to retrieve aerosol properties over surfaces such as arid, semi-arid and urban areas, where the surface reflectance in the blue spectral region is much darker than at longer wavelengths, with an estimated accuracy of 20–30 %. However, this approach is also restricted to certain geometric limitations because some assumptions do not apply to large solar zenith angles (SZA) or sensor zenith angles. In the Arctic region, the surface albedo can exceed 0.85 in areas covered by snow. Surface albedo is also a complicated function of surface and sub-surface optical properties, solar zenith angle, incident solar flux and cloud cover (Warren 1982; de Abreu et al., 1994). The longer path through the atmosphere at large viewing angles enhances the contribution of the signal reflected by aerosols (Wagner et al., 2010). Yet AOD retrieval over the Arctic is a great challenge. However, the aerosol optical depth and surface reflectance, which are determined simultaneously based on prior knowledge provide another way to obtain AOD with a bright surface (Wang et al., 2012). Holzer-Popp et al. (2002) developed a method to exploit data from both ATSR-2 (Along-track Scanning Radiometer 2) and GOME (Global Ozone Monitoring Experiment) for retrieval of aerosol properties (including AOD). In 2005, we proposed a new method by exploiting the synergy of TERRA and AQUA MODIS to accomplish part of the task of aerosol retrieval over land (Tang et al., 2005). It is obvious that there are many advantages by using synergy method, for example, it can provide more information for solving generally ill-posed or under-constrained Radiation Transfer Equations. However, more attention should be paid to the uncertainty causing by different platform. High-accuracy registration for different platforms is needed before retrieval process.

In this paper, an approach using both TERRA/MODIS and AQUA/MODIS data is presented. This new method is based on the operational bi-angle approach (Xue and Cracknell, 1995) to retrieve the AOD from MODIS data, which can describe the characteristics of the surface structure in some detail. This algorithm is introduced in detail in Sect. 2. The derived AOD is compared to Aerosol Robotic Network (AERONET) observations in the Arctic region in Sect. 4. Furthermore, the Russian wildfires occurred in late July of 2010, and their influence on the Arctic region was observed and analysed using ground and retrieval AOD data in Sect. 5.

2 Method

The basic equation for the transfer of radiation in plane-parallel atmospheres can be written in the following form (Kuznetzov, 1942):

$$\frac{\cos\theta'}{\rho}\frac{\delta I^{\lambda}(z,r)}{\mathrm{d}z}=\frac{\sigma}{4\pi}\int I^{\lambda}(z,r')\gamma^{\lambda}(z,r',r)\mathrm{d}\omega'-(\kappa+\sigma)I^{\lambda}(z,r) \tag{1}$$

where $I_{\lambda}(z,r)$ is the intensity of the radiation at height z and direction r. The other symbols are defined in the Appendix. The main concept of the most frequently used approximate radiative transfer equations consists of substituting the exact integrodifferential equation for radiant intensity by common differential equations for the upward and incident radiation fluxes.

Equation (1) can be decomposed into two differential equations: one for the upward flux (denoted as F_1), and the other one for the downward flux (denoted as F_2). These equations are as follows:

$$\frac{1}{\rho}\frac{\mathrm{d}F_1^{\lambda}(z)}{\mathrm{d}z}=-m_1^{\lambda}(z)\kappa F_1^{\lambda}(z)-m_1^{\lambda}(z)\sigma\Gamma_1^{\lambda}(z)F_1^{\lambda}(z)+m_2^{\lambda}(z)\sigma\Gamma_2^{\lambda}(z)F_2^{\lambda}(z) \tag{2}$$

$$-\frac{1}{\rho}\frac{\mathrm{d}F_2^{\lambda}(z)}{\mathrm{d}z}=-m_2^{\lambda}(z)\kappa F_2^{\lambda}(z)-m_2^{\lambda}(z)\sigma\Gamma_2^{\lambda}(z)F_2^{\lambda}(z)+m_1^{\lambda}(z)\sigma\Gamma_1^{\lambda}(z)F_1^{\lambda}(z) \tag{3}$$

where

$$m_1^{\lambda}(z)=\frac{\int_{2\pi^+}I_1^{\lambda}(z,r')\mathrm{d}\omega'}{\int_{2\pi^+}I_1^{\lambda}(z,r')\cos\theta'\mathrm{d}\omega'},\quad m_2^{\lambda}(z)=\frac{\int I_2^{\lambda}(z,r')\mathrm{d}\omega'}{\int I_2^{\lambda}(z,r')\cos\theta'\mathrm{d}\omega'}, \tag{4}$$

AMTD
4, 7597–7622, 2011

$$\Gamma_1^\lambda(z)=\frac{\int_{2\pi^-} I_1^\lambda(z,r')\beta_1^\lambda(r')\mathrm{d}\omega'}{\int_{2\pi^-} I_1^\lambda(z,r')\mathrm{d}\omega'}\,,\quad \Gamma_2^\lambda(z)=\frac{\int_{2\pi^+} I_2^\lambda(z,r')\beta_2^\lambda(r')\mathrm{d}\omega'}{\int_{2\pi^+} I_2^\lambda(z,r')\mathrm{d}\omega'}\,, \tag{5}$$

$$\beta_1^\lambda(r')=\frac{1}{4\pi}\int_{4\pi}\gamma_{1,2}^\lambda(z,r',r)d\omega\,,\quad \beta_2^\lambda(r')=\frac{1}{4\pi}\int_{4\pi}\gamma_{2,1}^\lambda(z,r',r)\mathrm{d}\omega\,, \tag{6}$$

$$\gamma_{1,2}^\lambda(z,r',r)=\gamma^\lambda(z,r',-r)\,,\quad \gamma_{2,1}^\lambda(z,r',r)=\gamma^\lambda(z,-r',r)\,, \tag{7}$$

$$I_1^\lambda(z,r)=I^\lambda(z,r)\,,\quad I_2^\lambda(z,r)=I^\lambda(z,-r)\,. \tag{8}$$

Xue and Cracknell (1995) using a two-stream approximation based on the assumption that the radiation attenuation is determined by the primary scattering influence only, then following equation can be obtained:

$$\frac{\mathrm{d}F_1^\lambda(z)}{\mathrm{d}\tau^\lambda}=-m_1^\lambda(z)\Gamma_1^\lambda(z)F_1^\lambda(z)+m_2^\lambda(z)\Gamma_2^\lambda(z)F_2^\lambda(z) \tag{9}$$

$$\frac{\mathrm{d}F_2^\lambda(z)}{\mathrm{d}\tau^\lambda}=-m_1^\lambda(z)\Gamma_1^\lambda(z)F_1^\lambda(z)+m_2^\lambda(z)\Gamma_2^\lambda(z)F_2^\lambda(z) \tag{10}$$

With the following boundary conditions for the upward and downward fluxes at the top and the bottom of the atmosphere,

$$\frac{F_1(\tau=0)}{F_2(\tau=0)}=R' \tag{11}$$

$$\frac{F_1(\tau=\tau_0)}{F_2(\tau=\tau_0)}=R \tag{12}$$

Therefore, we can find the relationship between the ground surface reflectance R and the apparent reflectance (reflectance at the top of the atmosphere) R', which is proposed as follows:

$$R=\frac{(bR'-\sec\theta)+\sec\theta(1-R')e^{(\sec\theta-b)\varepsilon\tau_0}}{(bR'-\sec\theta)+b(1-R')e^{(\sec\theta-b)\varepsilon\tau_0}}\,, \tag{13}$$

AMTD
4, 7597–7622, 2011

Where ε is the backscattering coefficient, typically 0.1, and τ_0 is the atmospheric optical depth, which consists of two parts: the molecular Rayleigh scattering (τ_m) and the scattering by aerosol particles (τ_A). The molecular scattering and the scattering by aerosol particles can be expressed as follows (Ångström, 1929):

$$\tau_A = \beta\lambda^{-\alpha} \tag{14}$$

where β is Ångström's turbidity coefficient, α is the Ångström coefficient, and λ is the wavelength. Xue and Cracknell (1995) suggested that $b = 2$ for most common cases. However, their experiment showed great variation when the solar zenith angle is larger than 60°, similar to that in the Arctic region; this finding may cause certain errors and error increase with increasing solar zenith angle. We used the following equation from Kondratyev (1969),

$$b = 0.21 \cdot \sec\theta + 1.78 \tag{15}$$

Equation (13) is not perfect when the solar zenith angle is near 60° because the general solution given by Kondratyev (1969) demonstrated that flux was not sensitive to AOD when the solar zenith angle is equal to 60°; however, it is common that the solar zenith angle is around 60° in the Arctic region. Actually most of the solar zenith angle is in the range of (60°–80°), taking MODIS as an example. Therefore, when SZA is equal to 60°, we put forward another equation as follows for the Arctic region to replace Eq. (13):

$$R = \frac{R' + \sec\theta\varepsilon\tau_0^{\lambda}\sec\theta'(R' - 1)}{1 + \sec\theta\varepsilon\tau_0^{\lambda}\sec\theta'(R' - 1)} \tag{16}$$

Flowerdew and Haigh (1995) proposed that the surface reflectance can be approximated by a part that describes the variation with the wavelength and a part that describes the variation with the geometry. Under this assumption, the ratio of the surface

AMTD
4, 7597–7622, 2011

reflectance from both TERRA/MODIS data and AQUA/MODIS data in a day can be expressed as follows:

$$K_{\lambda_i} = \frac{R_{1,\lambda_i}}{R_{2,\lambda_i}}, \tag{17}$$

Where R_{1,λ_i} stands for the surface reflectance with the TERRA overpass of the study area, and R_{2,λ_i} is the surface reflectance with the AQUA overpass. Equation (17) provides a method which requires a consistent relationship between geometrically corresponding pixels across the channels. It is still useful for non-homogeneity while function sampled by different look may be quite different. It shows that the grand mean absolute error with k-approximation is 3.8 % while Lambertian error is 14.5 % for predicted reflectance (Flowerdew and Haigh, 1995).

The time interval between Terra and Aqua over-passes is around 100 min (Key et al., 2003). Based on Eqs. (13) to (17), we assumed that for two-overpass observations within such short time interval the aerosol types and properties (α) do not change, but β (Ångström's turbidity coefficient) will be different, and three visible bands (0.47, 0.55 and 0.66 µm) of both TERRA/MODIS and AQUA/MODIS were used for retrieving AOD.

Generally speaking, TOA reflectance increase with the aerosol load over a dark surface while over a bright surface increasing aerosol load would cause darkening of the scene at visible band. There is a reflectance threshold divide the positive effect and negative effect of aerosol. The most important factors in the new method here are the surface and the solar zenith angle. In Fig. 1, AOD takes values of 0.0001, 0.1, 0.5, 1.0, 1.5, and 2.0 and sub-figures with different SZAs of 50°, 55°, 60°, 65° and 70°. The relative azimuth angle between sun and sensor has a common value of 35°. From Fig. 1, we can see that the reflectance threshold increase with the increase of solar zenith angle. The reflectance for melting snow is around 0.6 and for fresh snow is around 0.8 over Arctic region. In Arctic region, the solar zenith angle is commonly larger than 50°, even 55°, with the reflectance threshold around 0.8 according to Fig.1. The sensitivity study using both Eqs. (13) and (15) in Fig. 1 show that the new method can still

AMTD
4, 7597–7622, 2011

separate the contribution from aerosol and surface with a large solar zenith angle. It is important to note that these effects are only valid for the discussed geometry. This will provide a new way for AOD retrieval for bright areas with a large solar zenith angle in Arctic region.

3 Data

The datasets used in this study included satellite data and ground-based data. The satellite data included raw data, such as MODIS Level 1 data for AOD retrieval and Level 2 data, such as aerosol and cloud classification products, are used as prior knowledge. Ground-based data were AERONET sunphotometer data and meteorological data. The cloud classification product was used for the cloud mask and the other data or products could be used together for Arctic region AOD retrieval.

MODIS Level 1 data is available through the LAADS website (http://modis.gsfc.nasa.gov/data/). Terra's orbit around the Earth is timed such that it passes from north to south across the equator in the morning, while Aqua passes south to north over the equator in the afternoon. Level 1 data was used to derive aerosol properties and cloud classification products over both land and ocean. In addition, the corresponding atmospheric product of Level 2 could also be obtained from the LAADS website. Both Level 2 data products for cloud and AOD could be used as prior knowledge.

AERONET provides globally distributed observations of spectral AOD for three data quality levels: Level 1.0 (unscreened), Level 1.5 (cloud-screened), and Level 2.0 (cloud-screened and quality-assured). Data from six AERONET sites at high latitudes (latitude greater than 70°) in the region of interest during the period from 1 to 15 August 2010 were collected as prior data for AOD retrieval and to analyse the influence of the Russian wildfires on the Arctic region. Figure 2 shows the study area (40°–90° N, −180°–180° E), and the AERONET station was used for retrieval and further analysis. Table 1 shows the information regarding latitude, longitude and elevation of the selected AERONET sites.

Discussion Paper | Discussion Paper | Discussion Paper | Discussion Paper |

AMTD

4, 7597–7622, 2011

4 Results and validation

Results from our AOD retrieval method are shown here to illustrate the retrieval sensitivity of the 10-km AOD product in response to maximum AOD variations from 0.1 to 2.0, on 3 August 2010. The AOD retrieved by our method at 0.55 µm for the TERRA and AQUA overpasses on that day is shown in Fig. 3a,b. The spatial distribution of the aerosol optical depth in the Arctic region can be easily observed. The retrieval results clearly show that the AOD over Russia is higher than over other areas. The meteorological data show that the Russian wildfires occurring in late July were responsible for these high values. In fact, MODIS-retrieved AOD shows that this hazy area has a relatively high AOD (>1.0), with a maximum exceeding 3.0, even 5.0, thereby indicating a higher aerosol concentration in Western Russia. On 3 August 2010, the AOD values of the burning area were around 1.5.

In this work we followed the methodology described in Ichoku et al. (2002) for the validation analysis. Because the aerosol products and sun-photometer retrievals have different spatial resolutions and temporal intervals, it would be incongruous to compare single MODIS pixel values directly to AERONET point measurements (Ichoku et al., 2002). All of the figures below represent the collocated points for the events in which both the MODIS and the AERONET cloud-masking algorithms indicated that no clouds were present. Because the resolution of retrieval AOD is $10 \times 10\,km^2$, each collocated AERONET site (Table 1) was identified in each MODIS aerosol image using its latitude and longitude. We used three different window sizes of 1×1, 5×5 and $10 \times 10\,km^2$. The averaged AOD values of those windows were calculated. If the differences of three averaged AODs are small enough (less than 0.001), we used $1 \times 1\,km^2$ window size for the validation. Otherwise, the standard deviations of AODs for pixels in $5 \times 5\,km^2$ window size and $10 \times 10\,km^2$ window size were calculated. The window size with pixels with smaller standard deviation of AODs is used for the validation.

Besides, we averaged all AERONET AOD data before 12:00 noon as the AOD data for the comparisons with retrieved AOD data from Terra MODIS data. In the same

AMTD
4, 7597–7622, 2011

way, we averaged all AERONET AOD data after 12:00 noon as the AOD data for the comparisons with retrieved AOD data from Aqua MODIS data.

Thirty-one matches were found in which both AERONET and retrieval from MODIS data had AOD values during the period from 1–15 August 2010. Because the AOD value in the Arctic region is always low (less than 0.1), Istomina (2011) suggested that AERONET data with extreme values of the Ångström coefficient for 440–870 nm should not be taken into account (less than 0.5 and more than 2.0), and a comparison between retrieved AOD and AERONET values less than 0.2 was presented. In the paper, six AERONET sites were chosen for validation. For the six AERONET sites in August, we use the real composite MODIS images (http://ladsweb.nascom.nasa.gov/browse_images/global_browser.html) at 500 m resolution, and we also use the MODIS cloud product to distinguish cloud and snow/ice. Figure 4 shows the relationship between AERONET values and retrieval values at 550 nm at different Arctic stations with an correlation coefficient (RCC) of 0.7909 and Root-Mean-Square-Error (RMSE) of 0.0254. The results in Fig. 4 indicate that the algorithm, especially in retrieving aerosol optical thickness over Arctic regions, shows relatively good agreement with observation values. The non-zero intercepts in the regressions resulted from an improper representation of surface reflectance in the MODIS retrieval procedure while the deviation of the slopes from unity indicated a systematic bias (Ichoku et al., 2002).

The detailed comparisons between retrieval and AERONET AOD values for each station are shown in Fig. 5. Retrieval and AERONET AOD values are well correlated for most cases. In Fig. 5, there are basically three surface types, which are plant (Andenes, Barrow and Tiksi), bared soil (Ittoqqortoommiit and OPAL) and snow (Thule). It shows a notably high level of accuracy in Andenes (Norway), Barrow (USA), OPAL (Canada) and Ittoqqortoormiit (Greenland). Figure 5 reveals that the quality of the retrievals for stations located in Thule and Tiksi is much degraded if compared with the other stations. The correlation ship between satellite-derived AOD and AERONET AOD is 0.67 over snow, which is acceptable. For bared soil area, the correlation is also 0.67, while for plant, the correlation is 0.84. In this paper, we pay attention to the whole

AMTD
4, 7597–7622, 2011

Arctic region, which contains variety of surface type, so we did not validate the method by different surface type.

5 Applications

Because of the large area coverage, remote sensing provides a useful tool for long-term aerosol transport studies. We want to analyze the extreme event, that is Russian wildfire in August, 2010, and its effect to Arctic atmospheric environment. Regarding this topic, a biomass burning episode in Western Russia which influenced the Arctic region occurred in the summer of 2010. The background outside the smoke trajectory over the region with latitude less than 70° is less than 0.4 (Mei et al., 2011) while the background AOD over the region with latitude larger than 70° is less than 0.1. Figure 6 demonstrates the AOD distribution during four days in the study area (1, 5, 12 and 15 August 2010) with a resolution of $10 \times 10\,\mathrm{km}^2$. In fact, the fires began in late July 2010, and four periods were divided for further analysis. The plume from the fires began to affect the Arctic region from late July to 3 August 2010; the affected area became serious from 4 August to 7 August 2010; the third effected period extended from 8 August to 12 August 2010, and the epilogue of the fires ranged from 13 August to 20 August 2010. MODIS-retrieved AOD shows that this hazy area has a relatively high AOD (> 1.0), with a maximum exceeding 3.0, even 5.0, thereby indicating enhanced aerosol concentrations in Western Russia on 1 August 2010.

A significant smoke aerosol plume from the Russian forest fires was observed over Western Russia on 1 August, 2010. The obvious transport trajectory of the plume can also be obtained by the retrieval of the AOD map in this area (see Fig. 6, red line). One plume moved northward to the Arctic region and the other moved eastward to effect middle Russia.

AMTD
4, 7597–7622, 2011

6 Conclusions

The new aerosol optical depth retrieval method proposed in this paper shows potential to address aerosol retrieval over more highly reflective surfaces on land, even with a large solar zenith angle, which provides a way for Arctic region AOD retrieval. The validation also shows that the new method has a relatively high level of accuracy. But for some areas, the retrieval AODs are either overestimated or underestimated as compared with ground-based measurements. The possible reasons for this are aerosol and water vapour spectral absorption, the registration of two temporal images, subpixel cloud contamination and our assumptions on invariant Ångström coefficient α and the ratio K for compensating the ground surface bi-directional property effects. Also, the cloud effect may be the most important factor in the Arctic region. Although this preliminary validation is encouraging, the difference in wavelengths and the time differences of various collection methods make comparisons difficult, and further validation is needed.

List of symbols

Symbol	Description
A	The Earth's surface reflectance
A'	The Earth's system reflectance (apparent reflectance observed from space)
r	The direction (zenith angle, azimuth angle)
$I_\lambda(z,r)$	The intensity of the radiation at height$z$ and direction r
z	Height
α	The wavelength exponent in Ångström's turbidity formula

AMTD
4, 7597–7622, 2011

β	Ångström's turbidity coefficient
$\gamma_\lambda(z,r,r')$	The scattering function that characterize the scattered light intensity distribution in the direction (z,r,r')
ε	Backscattering coefficient
θ	Solar zenith angle
k	The coefficient of absorption
λ	Wavelength
ρ	The density of air
P	Air pressure a.s.l.
σ	The coefficient of scattering
τ	Optical depth
τ_R	Rayleigh optical depth
τ_a	Aerosol optical depth
ω'	Solid angle
S	The signal from the sun-monitoring radiometer
S_0	The sun signal at the top of the atmosphere when the earth-sun distance is 1 AU
R	The earth-sun distance
m	The relative air mass

Acknowledgements. This work was partly supported by the Ministry of Science and Technology (MOST) of China under Grant No. 2010CB950802, 2010CB950803 and 2008AA12Z109 and by MOST of China under Grant No. 2007CB714407. L. L. Mei would like to thank the Director Prize from the Institute of Remote Sensing Applications of Chinese Academy of Sciences. MODIS data were available through NASA MODIS LAADS. Many thanks are due to the PI investigators with the AERONET sites used in this paper.

References

Ackerman, T. P., Stemback, J. N., and Valero, F. P. J.: The importance of Arctic haze for the energy budget of the Arctic, in: Arctic Air Pollution, Cambridge University Press, Cambridge, 151–158, 1986.

Ångström, A.: On the atmospheric transmission of sun radiation and on dust in the air, Geograf. Ann., 11, 156–169, 1929.

Damoah, R., Spichtinger, N., Forster, C., James, P., Mattis, I., Wandinger, U., Beirle, S., Wagner, T., and Stohl, A.: Around the world in 17 days – hemispheric-scale transport of forest fire smoke from Russia in May 2003, Atmos. Chem. Phys., 4, 1311-1321, doi:10.5194/acp-4-1311-2004, 2004.

Deuze, J. L., Breon, F. M., Devaux, C., Goloub, P., Herman, M., Lafrance, B., Maignan, F., Marchand, A., Nadal, F., Perry, G., and Tanre, D.: Remote sensing of aerosols over land surfaces from POLDER-ADEOS-1 polarized measurements, J. Geophys. Res., 106, 4913–4926, 2001.

De Abreu, R. A., Key, J., Maslanik, J. A., Serreze, M. C., and LeDrew, E. F.: Comparison of in situ and AVHRR-Derived Broadband Albedo over Arctic Sea Ice, Arctic, 47, 288–297, 1994.

Diner, D. J., Martonchik, J. V., Kahn, R. A., Pinty, B., Gobron, N., Nelson, D. L., and Holben, B. N.: Using angular and spectral shape similarity constraints to improve MISR aerosol and surface retrievals over land, Remote Sens. Environ., 94, 155–171, 2005.

Flowerdew, R. J. and Haigh, J. D.: An approximation to improve accuracy in the derivation of surface reflectances from multi-look satellite radiometers, Geophys. Res. Lett., 22, 1693–1696, 1995.

Gatebe, C. K., King, M. D., Tsay, S. C., Ji, Q., Thomas, A. G., and Li, J. Y.: Sensitivity of off-nadir zenith angles to correlation between visible and near-infrared reflectance for use in remote sensing of aerosol over land, IEEE T. Geosci. Remote Sens., 39, 805–819, 2001.

Grey, W. M. F., North, P. R. J., Los, S. O., and Mitchell, R. M.: Aerosol optical depth and land surface reflectance from multi-angle AATSR measurements: global validation and intersensor comparisons, IEEE T. Geosci. Remote Sens., 44, 2184–2197, 2006.

Govaerts, Y. M., Wagner, S., Lattanzio, A., and Watts, P.: Joint retrieval of surface reflectance and aerosol optical depth from MSG/SEVIRI observations with an optimal estimation approach: 1. Theory, J. Geophys. Res., 115, D02203, doi:10.1029/2009JD011779, 2010.

Herber, A., Thomason, L. W., Dethloff, K., Viterbo, P., Radionov, V. F., and Leiterer, U.: Volcanic

AMTD

4, 7597–7622, 2011

Aerosol optical depth retrieval in the Arctic region

L. Mei et al.

perturbation of the atmosphere in both polar regions: 1991–1994, J. Geophys. Res., 101, 3921–3928, doi:10.1029/95JD02462, 1996.
Holzer-Popp, T., Schroedter, M., and Gesell, G.: Retrieving aerosol optical depth and type in the boundary layer over land and ocean from simultaneous GOME spectrometer and ATSR-2 radiometer measurements, 1, Method description, J. Geophys. Res., 107, AAC16-1–AAC16-17, doi:10.1029/2001JD002013, 2002.
Hsu, N. C., Tsay, S. C., King, M. D., and Herman, J. R.: Aerosol properties over bright reflecting source regions, IEEE T. Geosci. Remote Sens., 42, 557–569, 2004.
Ichoku, C., Chu, D. A., Mattoo, S., Kaufman, Y. J., Remer, L. A., Tanre, D., Slutsker, I., and Holben, B. N.: A spatio-temporal approach for global validation and analysis of MODIS aerosol products, Geophys. Res. Lett., 29, MOD1-1-MOD1-4, doi:10.1029/2001GL013206, 2002.
Istomina, L. G., von Hoyningen-Huene, W., Kokhanovsky, A. A., Schultz, E., and Burrows, J. P.: Remote sensing of aerosols over snow using infrared AATSR observations, Atmos. Meas. Tech., 4, 1133–1145, doi:10.5194/amt-4-1133-2011, 2011.
Kaufman, Y. J., Tanre, D., Remer, L. A., Vermote, E. F., Chu, A., and Holben, B. N.: Operational remote sensing of tropospheric aerosol over land from EOS moderate resolution imaging spectroradiometer, J. Geophys. Res., 102, 17051–17067, doi:10.1029/96JD03988, 1997.
Key, J. R., Santek, D., Velden, C. S., Bormann, N., Thépaut, J.-N., Riishojgaard, L. P., Zhu, Y. Q., and Menzel, W. P.: Cloud-drift and water vapor winds in the polar regions from MODIS, IEEE T. Geosci. Remote Sens., 41, 482–492, 2003.
Kim, Y., Hatsushika, H., Muskett, R. R., and Yamazaki, K.: Possible effect of boreal wildfire soot on Arctic sea ice and Alaska glaciers, Atmos. Environ., 39, 3513–3520, 2005.
Kondratyev. K. Y.: Radiation in the Atmosphere, Academic Press, New York, London, 1969.
Kuznetzov, E. S.: On the problem of approximate transfer equations in a scattering and absorbing medium, Rep. Acad. Sci. USSR, 37, Nos 7 and 8, 1942.
Levy, R. C., Remer, L., Mattoo, S., Vermote, E. F., and Kaufman, Y. J.: Second-generation algorithm for retrieving aerosol properties over land from MODIS spectral reflectance, J. Geophys. Res., 112, D13211, doi:10.1029/2006JD007811, 2007.
Martonchik, J. V., Kahn, R. A., and Diner, D. J.: Retrieval of aerosol properties over land using MISR observations, in: Satellite Aerosol Remote Sensing Over Land, published in association with Praxis Publishing, Chichester, 267–268, 2009.
Mei, L., Xue, Y., de Leeuw, G., Guang, J., Wang, Y., Li, Y., Xu, H., Yang, L., Hou, T., He, X., Wu, C., Dong, J., and Chen, Z.: Integration of remote sensing data and surface observations

to estimate the impact of the russian wildfires over Europe and Asia during August 2010, Biogeosciences Discuss., 8, 7741–7790, doi:10.5194/bgd-8-7741-2011, 2011.
Remer, L. A., Wald, A. E., and Kaufman, Y. J.: Angular and seasonal variation of spectral surface reflectance rations: implications for the remote sensing of aerosol over land, IEEE T. Geosci. Remote Sens, 39, 275–283, 2001.
Remer, L. A., Kaufman, Y. J., Tanre, D., Mattoo, S., Chu, D. A., Martins, J. V., Li, R. R., Ichoku, C., Levy, R. C., Kleidman, R. G., Eck, T. F., Vermote, E., and Holben, B. N.: The MODIS aerosol algorithm, products, and validation, J. Atmos. Sci., 62, 947–973, 2005.
Remer, L. A., Tanré D., and Kaufman Y. J.: Algorithm for Remote Sensing of Tropospheric Aerosol from MODIS: Collection 5, ATBD_MOD_02.pdf, 1 November 2006, http://modis.gsfc.nasa.gov/data/atbd/atmos_atbd.php, last access: 10 October 2011, 2006.
Shaw, G. E.: The Arctic haze phenomenon, B. Am. Meteorol. Soc., 2403–2413, 1995.
Santer, R., Carrere, V., Dubuisson, P., and Roger, J. C.: Atmospheric corrections over land for MERIS, Int. J. Remote Sens., 20, 1819–1840, 1999.
Tang, J., Xue, Y., Yu, T., and Guan, Y.: Aerosol optical thickness determination by exploiting the synergy of TERRA and AQUA MODIS, Remote Sens. Environ., 94, 327–334, 2005.
Veefkind, J. P., de Leeuw, G., and Durkee, P. A.: Retrieval of aerosol optical depth over land using two-angle view satellite radiometry during TARFOX, Geophys. Res. Lett., 25, 3135–3138, 1998.
Wang Y., Xue, Y., Li, Y. J., Guang, J., Mei, L. L., Xu, H., and Ai, J. W.: Prior knowledge supported aerosol optical depth retrieval over land surface at 500 m spatial resolution with MODIS data, Int. J. Remote Sens., 33, 674–691, 2012.
Warren, S. G.: Optical properties of snow, Rev. Geophys. Space Phys., 20, 67–89, doi:10.1029/RG020i001p00067, 1982.
Wagner, S. C., Govaerts, Y. M., and Lattanzio, A.: Joint retrieval of surface reflectance and aerosol optical depth from MSG/SEVIRI observations with an optimal estimation approach: 2. Implementation and evaluation, J. Geophys. Res., 115, D02204, doi:10.1029/2009JD011780, 2010.
Xue, Y. and Cracknell, A. P.: Operational bi-angle approach to retrieve the Earth surface albedo from AVHRR data in the visible band, Int. J. Remote Sens., 16, 417–429, 1995.

Table 1. Six selected AERONET stations in the Arctic region and their location (latitude and longitude) selected for our aerosol retrieval validation.

Number	Name	Longitude (° East)	Latitude (° North)	Altitude(m)
1	Andenes	16.008 611	69.278 333	379
2	Barrow	−156.665	71.312 2	0
3	Ittoqqortoormiit	−21.951 2	70.484 8	68
4	OPAL	−85.939 167	79.990 278	0
5	Thule	−68.769 001	76.516 102	225
6	Tiksi	128.921 417	71.586 917	0

AMTD
4, 7597–7622, 2011

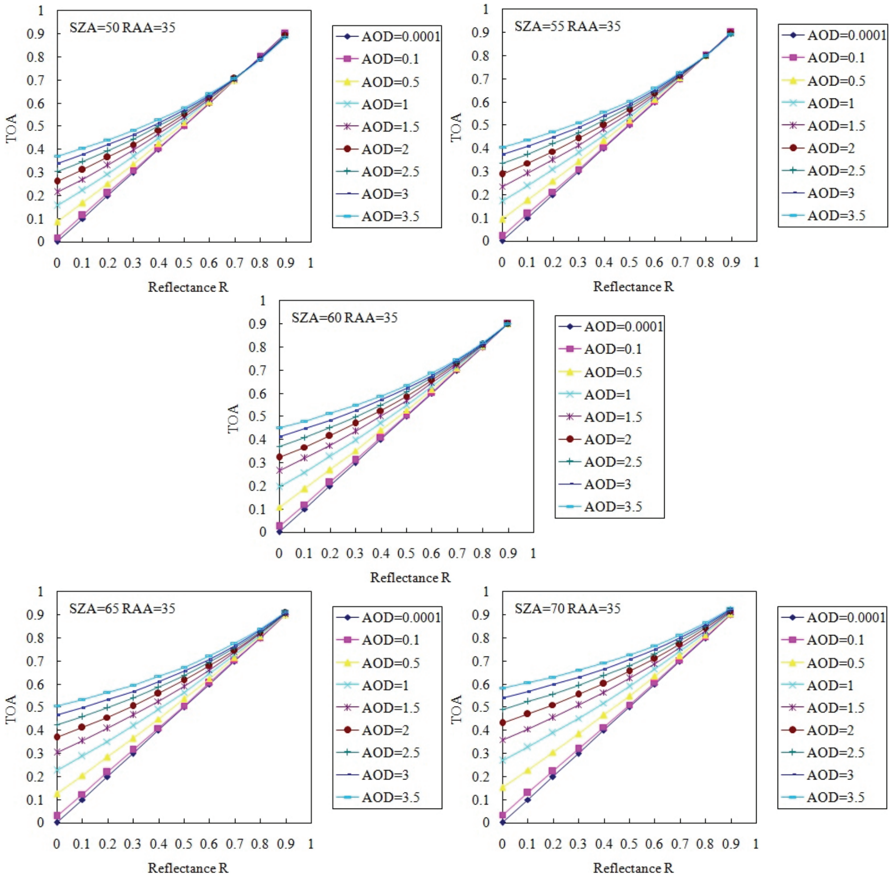

Fig. 1. Sensitivity analysis of combination of Eqs. (13) and (15) with Solar Zenith Angle (SZA) of different AODs. RAA is the relative azimuth angle between the Sun and the satellite sensor. TOA is the reflectance R' at the top of the atmosphere.

AMTD
4, 7597–7622, 2011

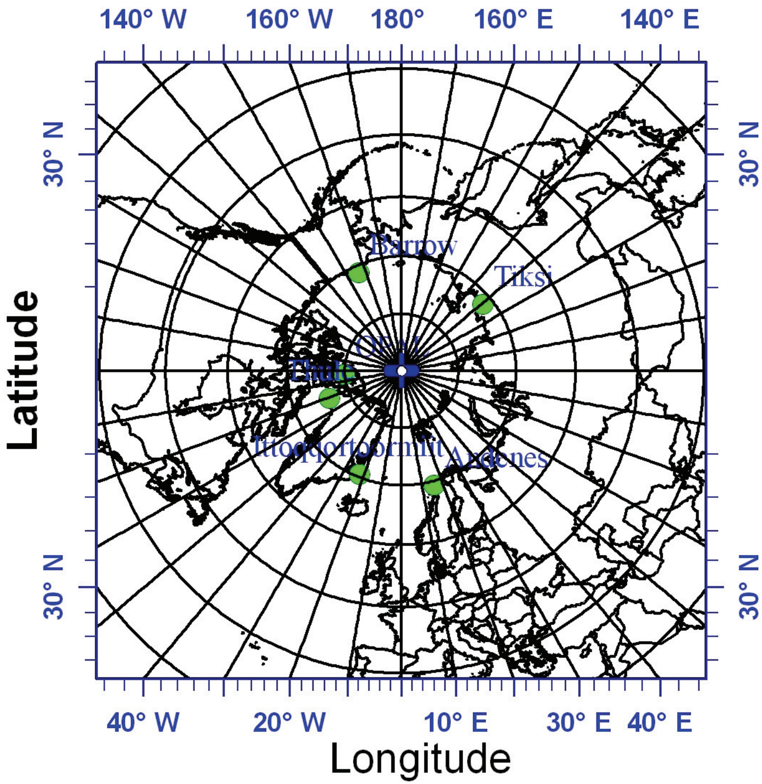

Fig. 2. Study area and AERONET sites (green points) located in the area.

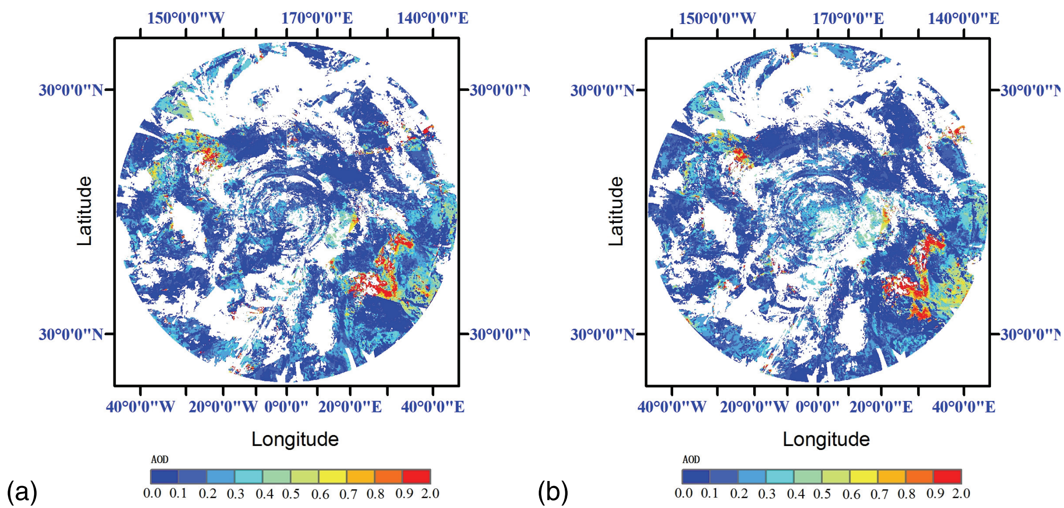

Fig. 3. Aerosol optical depth derived at 550 nm of the TERRA/AQUA overpass with 10 km resolution on 3 August 2010, using the method described in Sect. 2: **(a)** TERRA; **(b)** AQUA.

AMTD
4, 7597–7622, 2011

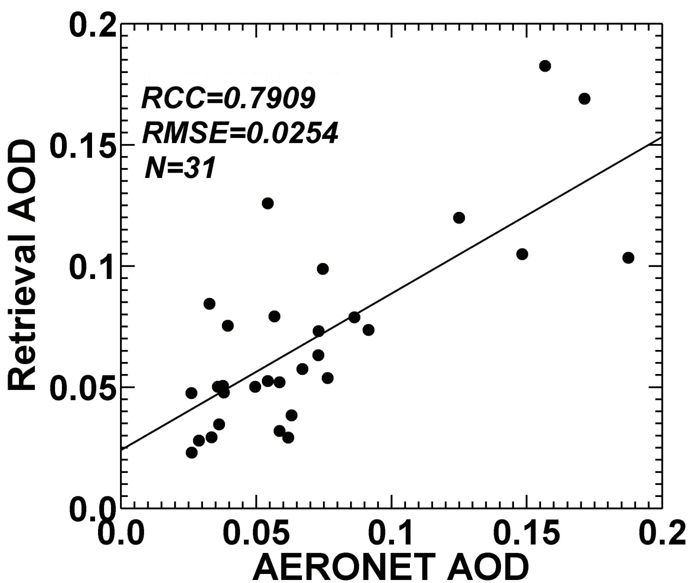

Fig. 4. Relationship between AODs derived from MODIS data with $10 \times 10\,\text{km}^2$ resolution and AODs from AERONET observation at 500 nm during 1 and 15 August 2010 by the new method at six Arctic stations. Here, RCC stands for correlation coefficient, RMSE means root-mean-square error and N is total number of matched cases.

AMTD
4, 7597–7622, 2011

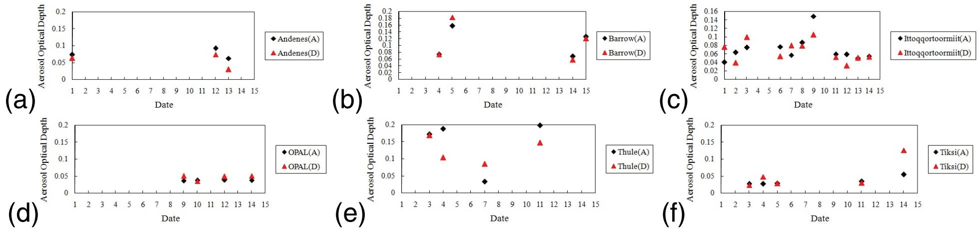

Fig. 5. Time series of AODs during 1 and 15 August 2010 at different AERONET stations: **(a)** Andenes; **(b)** Barrow; **(c)** Ittoqqortoormiit; **(d)** OPAL; **(e)** Thule; **(f)** Tiksi (A stands for AERONET, and D stands for derived from satellite data).

AMTD
4, 7597–7622, 2011

Aerosol optical depth retrieval in the Arctic region

L. Mei et al.

Title Page
Abstract
Introduction
Conclusions
References
Tables
Figures
◀
▶
Back
Close
Full Screen / Esc
Printer-friendly Version
Interactive Discussion

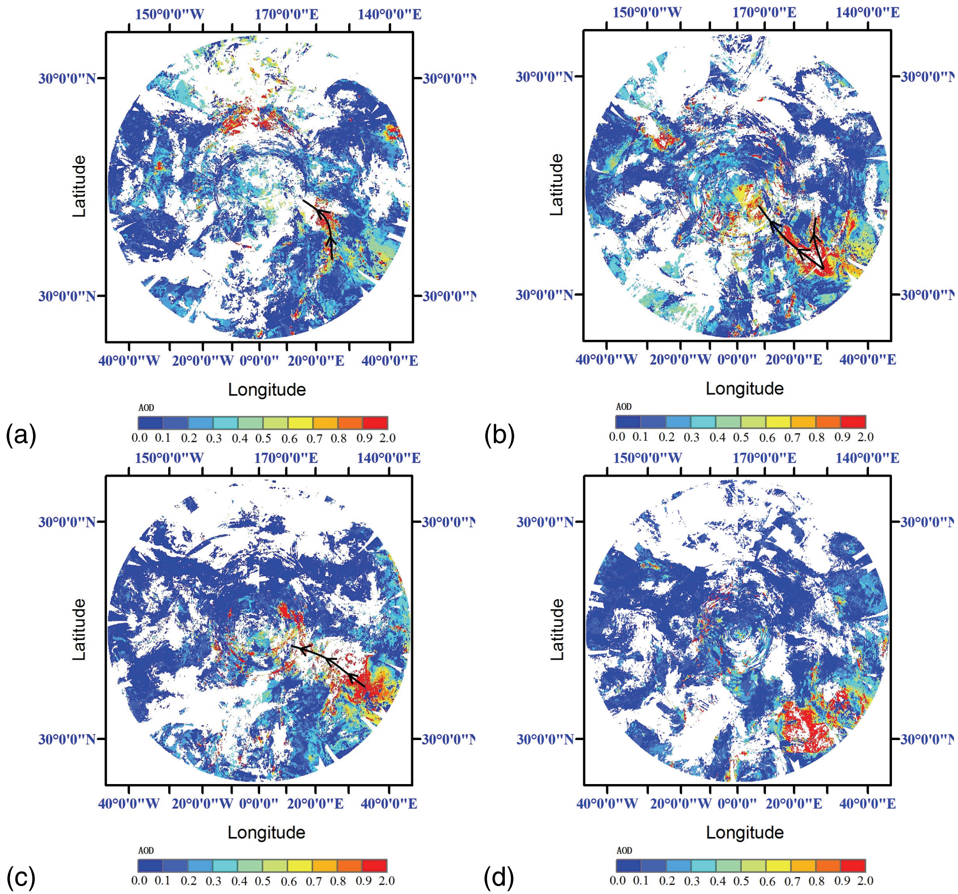

Fig. 6. AOD distribution and its trajectory in the study area during the Russian wildfires: **(a)** 1 August 2010; **(b)** 5 August 2010; **(c)** 12 August 2010; **(d)** 15 August 2010.

AMTD
4, 7597–7622, 2011

Aerosol optical depth retrieval in the Arctic region

L. Mei et al.